

The Search for a Highly Efficient Long-Wavelength Photoinitiator by Increasing Aryl Conjugation: From
Computational Design, Characterization, and Potential Application

Justine S. Wagner

April 6, 2015

University of Colorado at Boulder

Department of Biochemistry

Honors Council Representative:

Joseph Falke, Department of Chemistry and Biochemistry

Primary Thesis Advisor:

Dr. Christopher Bowman, Department of Chemical and Biological Engineering

Committee Members:

Dr. Joseph Falke, Department of Chemistry and Biochemistry

Dr. Christopher Bowman, Department of Chemical and Biological Engineering

Dr. Nancy Guild, Department of Molecular, Cellular, and Developmental Biology

Dr. Jennifer Kugel, Department of Chemistry and Biochemistry

Table of Contents

Abstract.....	3
Acknowledgements.....	4
Introduction to Photoinitiators.....	5-6
Particles in a Box.....	6-7
Molecular Orbital Theory.....	7-8
Introduction to APO and BAPO.....	8
Properties and Photochemistry of Acylphosphine Oxide (APO).....	8-9
Properties and Photochemistry of Bisacylphosphine Oxide (BAPO).....	9-10
Scope of Research.....	10-11
Experimental Design.....	11
Instrumentation and Materials.....	11
Procedure.....	12-14
Computational Studies.....	15-16
Results.....	17
Nuclear Magnetic Resonance (NMR).....	17-22
Mass Spectrometry.....	22-25
UV-vis Spectroscopy.....	26-27
Infrared (IR) Spectroscopy.....	27-30
Real-Time UV-vis	31
Photo-bleaching.....	31-33
Discussion.....	33-36
Conclusion and Future Scope.....	36-38
References.....	39-40

Abstract

Currently, dental composites are limited to layer-by-layer deposition due to depth curing limitations using blue light. In dental composites, monomers are polymerized by light with the presence of photoinitiators (PI). Free-radicals, which promote polymerizations of vinyl monomers, are formed when PIs are excited by irradiation (either UV or visible light). A widely used photoinitiating system in the dental industry consists of a combination of camphorquinone and ethyl 4-dimethylaminobenzoate. The drawback in the usage of this method is the yellow coloring and stability of these PIs. There is a current demand for a PI that initiates curing in the visible light with high efficiency. This demand is not only needed in the dental industry, but also in fields such as laser 3D printing and regenerative medicine. In this study, three new photoinitiators (2-Naphthacene (APO), 9-Anthracene (APO), and 9-Anthracene (BAPO)) were synthesized, characterized, and evaluated for its potential application for visible light curing. UV-vis spectroscopy results show that increasing the aromaticity of the PI increases the wavelength of absorption as well as the molar extinction coefficient. However, IR kinetics and Real Time UV-vis spectroscopy results show that the efficiency of the radicals from the photoinitiators are drastically infringed based on the stabilization effect occurring on the radicals. These above mentioned PIs can help us understand the design of a PI with greater efficiency in the visible light curing. In addition, they may potentially replace the current initiating systems used in the dental industry as well as other photochemistry based fields.

Acknowledgements

I would like to give my sincere appreciation to Dr. Tao Gong who originally accepted me in Dr. Bowman's research lab, and was my research mentor from the beginning of the photoinitiator project. In addition, I would like to thank graduate student Chern-Hooi Lim whom, once Dr. Gong left, became my supportive and professional growth mentor, as well as Dr. Charles Musgrave. I would like to thank Dr. Nancy Guild and Dr. Jennifer Kugel whom accepted to be part of my research committee even though I was bringing them out of their comfort zone do to the less biology standpoint of my research. I would like to extend that thank you to Dr. Joseph Falke and Dr. Christopher Bowman who invested their time to critique my honors thesis draft and provided guidance. I would like to give my gratitude to members of the Bowman and Stransbury group who supported me along the way. They also provided insight in synthetic and experimental results, as well as critiquing my thesis draft (graduate students Chen Wang and Weixian Xi). Lastly but certainly not the least, I would like to thank Dr. Christopher Bowman who allowed me to perform my honors thesis in his lab as well as allowed me to continue conducting research as an independent undergraduate researcher. Without everyone's acceptance and involvement I would never have achieved my level of professional growth which may still be mediocre to this day but will eventually reach a level that I would originally have not thought possible.

Introduction to Photoinitiators

Over the last few decades, photochemistry has been used in the field of dental materials for the photo-curing of methacrylate monomers. Photochemistry is a method that promotes specific bonds of methacrylate monomers to crosslink to form a polymer. The current applications on the usage of photochemistry in the dental field are the photo-curing of composite restoratives, liquid bonding agents to help repair cavities, and orthodontic bracket adhesives (Kilian, 1981). A typical photo-initiated dental material is comprised of a monomer, a diluent, a photoinitiator, and inorganic filler (Schuster et al., 2005). The search for a visible light curing photoinitiator system is of high demand in the dental industry as well as other fields that utilize photochemistry such as regenerative medicine and laser-induced 3D printing.

The polymerization of dental composites is greatly restricted due to the sensitivity of the oral cavity. Polymerization should be safe (pH and toxicity) and not exceed 50°C to protect the oral tissue from damage. This imposing restriction prevents the usage of thermally initiated free-radical polymerizations as a usage of curing dental composites. In addition to temperature sensitivity, the oral tissues are sensitive to the formation of acids that occur in ionic polymerization systems initiated at room temperature (Linden, 1993). A solution that can be currently presented to overcome these problems is the usage of photo-curing radical polymerization.

Photo-curing polymerization is an efficient method for curing monomers. Photoinitiators are the primary components that promote the crosslinking of unsaturated monomers. Most photoinitiators absorb light in the far UV spectrum to form organic radicals (Schafer et al, 2004). The formation of the unstable radicals initiates the crosslinking of alkenes by radical addition processes. A common issue that must be addressed/considered when choosing a photoinitiator is the maximum absorption wavelength (λ_{\max}), the molar extinction coefficient (ϵ) of the photoinitiator, and the dissociation efficiency of the photoinitiators, which all determine general applicability (Sobhi, 2005).

The photoinitiators λ_{\max} used should correlate with the spectral emission profiles of the dental lamp in usage. The combination of the photosensitizer camphorquinone (CQ) and co-initiator ethyl 4-dimethylaminobenzoate is widely used in dental resin and adhesive formulations (Musanje et al., 2009). CQ is a yellow powder that is hard to bleach which results in large amounts of CQ left in resin creating an undesirable yellowing in the final appearance of the cured material (Neumann, 2005).

The photoinitiators absorptivity is a fundamental standpoint in improving the photochemical reaction efficiency. It is essential to select photoinitiators with absorption spectra that overlap with the emission spectra of the lamp. In Light Emitting Diode (LED) curing lights, the broad emission spectrum ranges from 380 to 515 nm with maximum emission between 460-480 nm (3M ESPE, 2002). A large molar extinction coefficient (ϵ) indicates a high probability of absorption at a given wavelength, leading to large quantum yields of the initiating free-organic radicals. (Neumann, 2005). Understanding the free radical polymerization process should lead to more efficient polymer production, saving both time and money, less waste and new polymer products (Hristova, 2005).

Particles in a Box

When a molecule absorbs a photon, the electron jumps from one energy level, n_i , to a higher energy level, n_f . The particle in a one-dimensional box model is a quantum mechanical model that predicts the energy levels for conjugated molecules. When light energy is exposed to a conjugated molecule and the light energy matches the transition within the molecule, some of the energy will be absorbed as the electron is promoted to a higher energy orbital and some of the energy will be lost due to internal conversion and intersystem crossing. Conjugation of double and triple bonds shifts the absorption maximum to longer wavelengths and the molar absorptivity (ϵ) roughly doubles with each new conjugated double bond (de Dios, 2014).

Molecules with conjugated double bonds have energy levels that are more closely spaced than molecules in comparison to only single bonds. Conjugation will result in less energy needed in order to

promote electrons from ground state to excited state. This will result in greater absorption of photons of a lower energy and frequency to which this energy corresponds to the visible portion of the electromagnetic spectrum.

In order to consider the one-dimensional box model, the potential energy of one electron is constant throughout box and rises to infinity at each end of the conjugated (de Dios, 2014). Schrödinger's equation can be applied leading to the wave function equation:

$$\Psi_n = \sqrt{\frac{2}{L}} \sin\left(\frac{n\pi x}{L}\right) \text{ and } E_n = \frac{n^2 h^2}{8mL^2}$$

X is the displacement along the backbone and L corresponds to the length of the conjugated molecule. Each wave function can be regarded as a molecular orbital, and the energy is the orbital energy (de Dios, 2014). However, in the case of photoinitiators, one has to take into consideration of many-electron atoms which becomes challenging and tedious to calculate. Luckily, there are high-speed computers which enable the orbitals of many-electron atoms to be computed as well as the absorption wavelength.

Molecular Orbital Theory

Molecular orbital theory is useful in explaining the aromatic properties which can be applied to photoinitiators. Molecular orbital calculations provide the lowest and highest energy MOs (Ψ and Ψ^*), bonding and anti-bonding energy levels. As the conjugated pi systems increases, the energy gap between $\pi - \pi^*$ transition becomes narrow which leads to an increase in longer wavelength absorption (Soderberg, n.d.). Figure 1 demonstrates that as the aromatic ring increases the energy gap becomes increasingly smaller. The decrease in energy gap leads to easy promotion of the electron from one energy level to a higher energy level. As aryl conjugation increases, the HOMO-LUMO gap starts to become narrow to which the wave function overlap grows exponentially leading to stabilization of the LUMO and destabilization of the HOMO. This is demonstrated in the spectroscopic properties of Anthracene, Naphthacene, and Benzene having a λ_{\max} at 357, 315, and 255 nm, respectively.

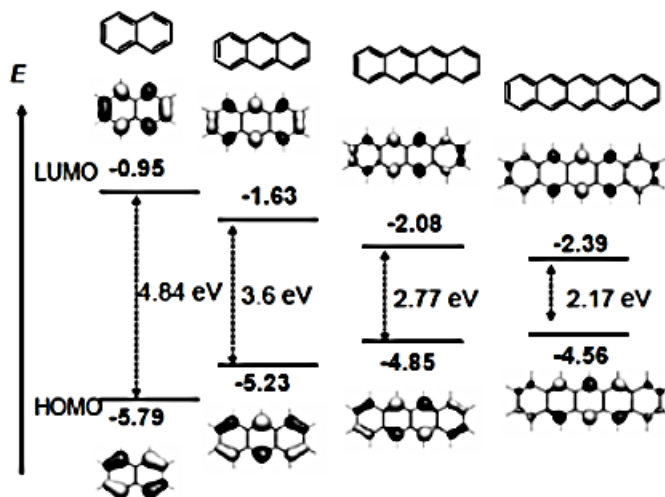


Figure 1. HOMO-LUMO Gap of Oligoacenes (Shinamura, 2011).

Introduction to APO and BAPO

Properties and Photochemistry of Acylphosphine Oxide (APO)

Acylphosphine oxides (APO) are photoinitiators that undergo homolytic α -cleavage at the carbonyl-phosphorus bond to generate two free organic radicals; Figure 2 demonstrates the overall process. Both of the free radical species are capable of initiating polymerization but with different rate constants. The absorption characteristics of APO typically show enhanced absorption in the near UV/visible range. The absorption maxima is around 350-380 nm and tails around the 420 nm region (Hristova, 2005). The long wavelength absorption is due to the $n\text{-}\pi^*$ transition (Spichy et al., 2001).

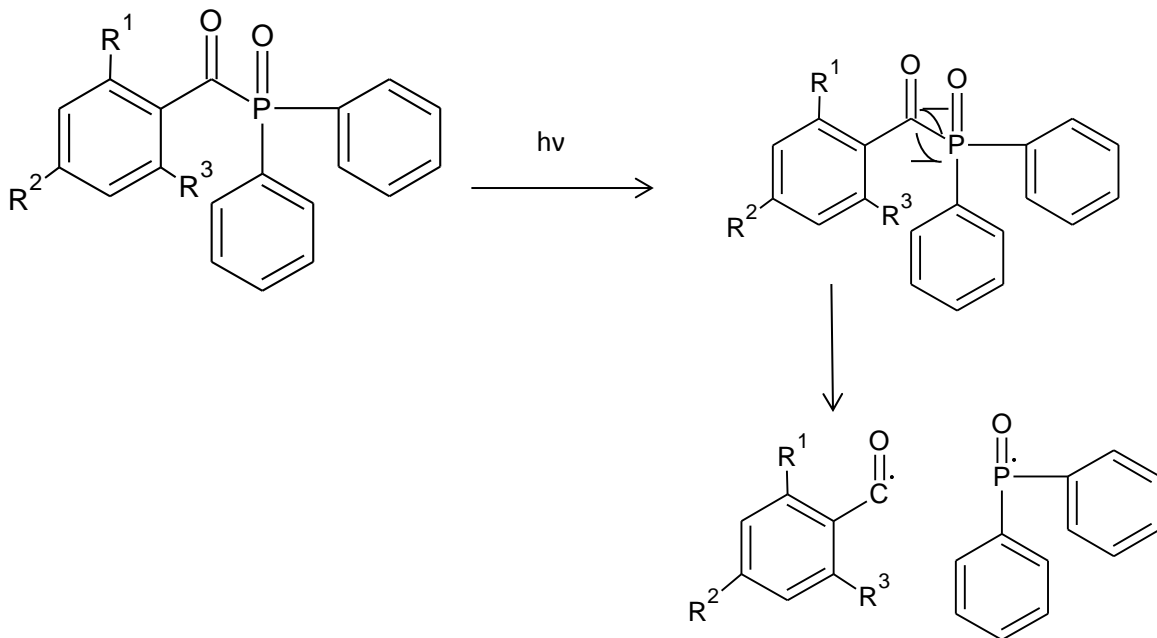


Figure 2. Schematic that demonstrates the α -cleavage that occurs for APO photoinitiators.

Properties and Photochemistry Bisacylphosphine Oxide (BAPO)

Bisacylphosphine Oxide (BAPO) is a photoinitiator that also undergoes homolytic α -cleavage at the carbonyl-phosphorus bond to generate two free organic radicals; Figure 3 demonstrates the overall process. Both of the free radical species are capable of initiating polymerization but with different rate constants. BAPO exhibits UV-near-visible absorption around 350–380 nm extending up to 420–440nm. In addition, BAPO have molar extinction coefficients around $300\text{--}800\text{ mol}^{-1}\cdot\text{cm}^{-1}$ which is very high compared to APO derivatives. The high absorption corresponds to the $n \rightarrow \pi^*$ HOMO–LUMO transition because of the conjugation with the phosphoryl group that occurs on both sides which enhances the overall property of the BAPO (Fouassier and Lalevee, 2012).

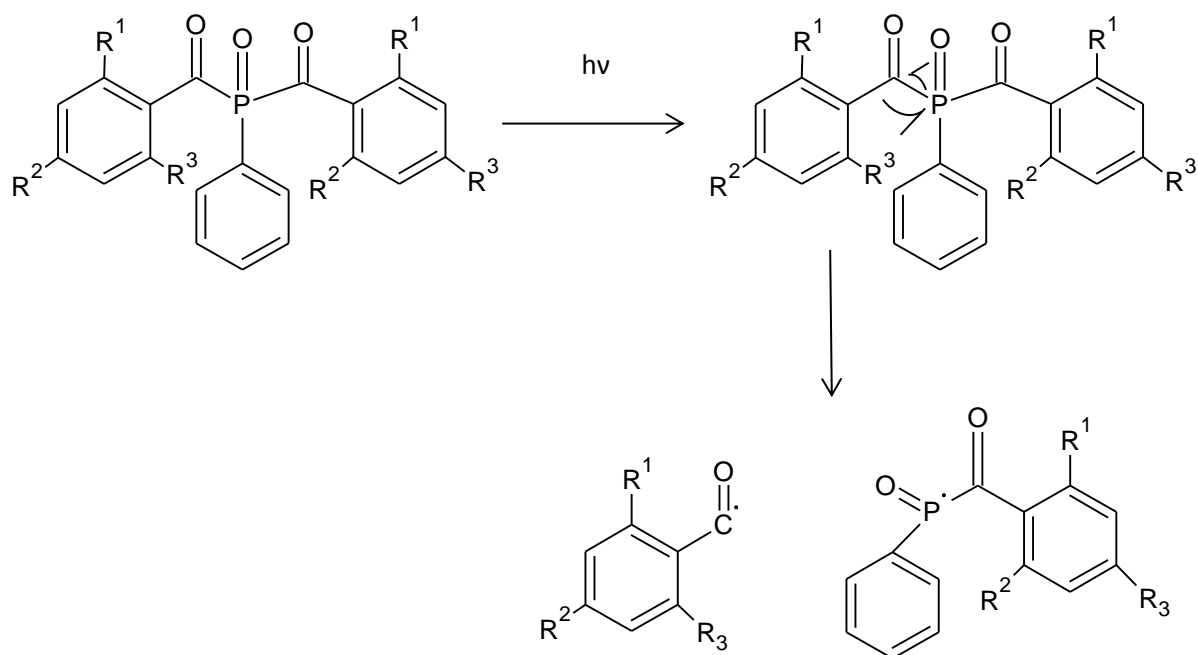


Figure 3. Schematic the displays the α -cleavage that occurs for BAPO photoinitiators.

Scope of Research

The overall scope of this research is to computationally design and synthesize new photoinitiators, comprised of APO and BAPO derivatives, which are red-shifted from conventional UV absorption to visible light absorption. The hypothesis is that these novel photoinitiators will be suitable for dental composites when the commercial LED-dental lamps emission wavelength overlaps the absorption wavelength (specifically the λ_{max}) of the photoinitiators. Moreover, a photoinitiator that photo-bleach during photo-polymerization would be beneficial and also lead to an increase in curing depth as well as preventing less desirable cosmetic appearance. Based on the principle of particle in a box and molecular orbital diagrams, decreasing the energy gap between $\pi - \pi^*$ transition leads to an increased absorption at longer wavelength. This can occur by increasing conjugation of the aryl ring which will also increase the molar extinction coefficient. Therefore, creating new photoinitiators (2-

naphthacene (APO), 9-anthracene (APO), and 9-anthracene (BAPO)) will demonstrate a general proof of concept that molar extinction coefficient and wavelength absorption will increase, but how this will affect the photoinitiator ability to cleave and generate radicals that will initiate polymerization will be investigated.

Experimental Design

Instrumentation and Materials

General. ^1H , ^{13}C , ^{31}P NMR spectra recorded with Bruker Avance-III 400 MHz spectrometer. Low Resolution Electrospray Ionization (ES+) measured with Thermo Finnigan LTQ Orbitrap that is operated in the central laboratory at the University of Colorado at Boulder. Column Chromatography was performed using Teledyne Isco CombiFlash RF-200 Automated Flash Chromatography. UV-vis spectrum was measured with UV-vis spectrometer from Thermo-Fischer Scientific Evolution 300 series. Conversion of Samples and IR spectrum of solid samples were measured using Thermo-Fisher Scientific Nicolet FT-IR 6700 spectrometer. CDCl_3 was used as the standard solvent for field stabilization in NMR measurements. EXFO Acticure Mercury 4000 UV Cure Arc Lamps were used with 400-500 nm and 365 nm light filters.

Materials. Benzoyl chloride (99%), 2-Naphthoyl chloride (98%), 9-Anthracene carboxylic acid (99%), Tert-butanol ($\geq 99\%$), Sodium (99%) containing Kerosene, Toluene (99.8%), N,N-Dimethylformamide (99.8%), Methyl diphenylphosphinite (97%), P,P-Dichlorophenylphosphine (97%), and Triethylene glycol diacrylate were obtained from Sigma Aldrich. Sodium bicarbonate and 30% Hydrogen peroxide were purchased from Fischer Scientific.

Procedure

Acylphosphine Oxide (APO) Derivative Synthesis

Synthesis of (diphenylphosphoryl)(phenyl)methanone. To a 25 mL flame-dried, round bottom flask, Benzoyl chloride (0.500 g, 3.56 mmol) and 10 mL of anhydrous Toluene were added. After stirring for 5 minutes, Methyl diphenylphosphinite (0.714 mL, 3.56 mmol) was carefully added to the solution. The stirring mixture was then immediately wrapped with aluminum foil to prevent any light exposure and placed on an oil bath at 70°C for 24 hours. The solution had a faint yellow appearance. The solution was then rotovaped to complete dryness and the crude product was run through a column using gradient DCM:MeOH. After collecting the product, the residue was dried in vacuo giving 0.870 g (80% yield) of a light yellow wax consisting of $C_{19}H_{15}O_2P$ (Benzene PI).

Synthesis of (diphenylphosphoryl)(naphthalene-2-yl)methanone: To a 50 mL flame-dried, round bottom flask, 2-Naphthoyl chloride (0.500 g, 2.62 mmol) and 10 mL of anhydrous Toluene were added. After stirring for 5 minutes, Methyl diphenylphosphinite (0.530 mL, 2.62 mmol) was carefully added to the solution. The solution immediately turned faint yellow in appearance. The stirring mixture was then immediately wrapped with aluminum foil to prevent any light exposure and placed on an oil bath at 70°C for 24 hours. The mixture was then rotovaped to complete dryness and the crude product was run through a column using gradient DCM:MeOH. After collecting the product, the residue was dried in vacuo giving 0.578 g (62% yield) of a light yellow powder consisting of $C_{23}H_{17}O_2P$ (2-Naphthoyl PI).

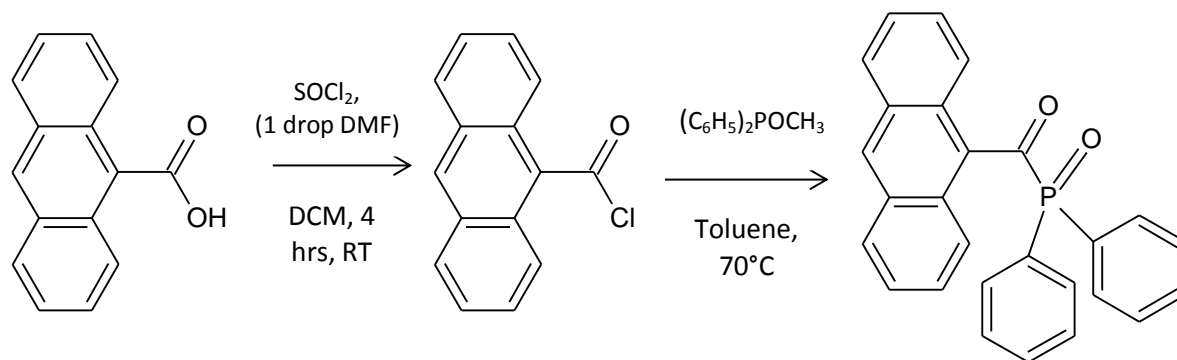


Figure 4. Synthesis of 9-Anthracene APO PI

Synthesis of (diphenylphosphoryl)(anthracene-9-yl)methanone: To a 50 mL flame-dried, round bottom flask, 9-Anthracene carboxylic acid (0.500 g, 2.25 mmol) and 25 mL of anhydrous Dichloromethane were added. After stirring for 10 minutes, Thionyl chloride (0.163 mL, 2.25 mmol) was added drop wise and 1 drop of N,N-Dimethylformamide, as a catalyst, was immediately added afterwards. The solution then stirred at room temperature for 4 hours and afterwards rotovaped to complete dryness. The residue was further dried in vacuo. Assuming a 100% yield of 9-Anthroyl chloride ($C_{15}H_9ClO$), the yellow powder was re-dissolved in anhydrous Toluene. After stirring for 5 minutes, Methyl diphenylphosphinite (0.416 mL, 2.25 mmol) was carefully added to the solution. The solution immediately turned a deep yellow-gold in appearance. The stirring mixture was then immediately wrapped with aluminum foil to prevent any light exposure and placed on an oil bath at $70^{\circ}C$ for 24 hours. The mixture was then rotovaped to complete dryness and the crude product was run through a column using gradient DCM:MeOH. After collecting the product, the residue was dried in vacuo giving 0.640 g (70% yield) of a bright yellow powder consisting of $C_{23}H_{17}O_2P$ (9-Anthracene PI).

Synthesis of Bisacylphosphine Oxide (BAPO) Derivative

9-Anthracene (BAPO) was synthesized in a multi-step process according to the patent of Reinhard H. Sommerlade (Sommerlade et al., 2006).

Synthesis of Phenylbis(9-anthroyl)phosphine oxide:

Step 1: Methylation of P,P-dichloropenylphosphine

Excluding moisture by an Argon atmosphere, sodium lumps (1.00 g, 43.50 mmol) are suspended at room temperature in Anhydrous Toluene in a 250 mL flame-dried, 2-neck round bottom flask. Suspension is heated up to reflux with vigorous stirring once temperature reaches 98°C. P,P-dichlorophenylphosphine (1.41 mL, 10.89 mmol) was added drop wise under vigorous stirring. The reaction was left to continuously heat at reflux and stir for an additional 16 hours leading to the formation of a dark green solution.

Step 2: Protonation/Reduction

The dark green suspension was then treated with Tert-Butanol (2.08 mL, 21.75 mmol) while vigorously stirring at reflux temperature. Solution was left to stir for 1 hour.

Step 3: Acylation

The temperature was reduced to 35-37°C, and 9-Anthroyl chloride (5.23 g, 21.75 mmol) was added drop wise to the solution. The solution was wrapped with aluminum foil to prevent any light exposure and left to stir for 1 hour.

Step 4: Oxidation

The temperature was increased to 50°C and 30% Hydrogen Peroxide (1.00 mL, 32.63 mmol) was added by drop wise to the solution. The solution was recovered with aluminum foil and left to stir for 2.5 hours. Afterwards, 15 mL of a 5% aqueous NaHCO₃ solution was added and the mixture was left to stir for 10 minutes. The mixture was then transferred to a separatory funnel where the organic phase was collected and washed 3x with distilled H₂O. The solution was then rotovaped to complete dryness and the crude product was run through a column using gradient DCM: MeOH. After collecting the product, the residue was dried in vacuo giving 3.80 g (70% yield) of a bright yellow powder consisting of C₂₈H₁₉O₃P (9-Anthracene BAPO PI).

Computational Studies

The quantum chemical, computational prediction of the photoinitiators absorption wavelength was conducted by graduate student Chern-Hooi Lim in Dr. Charles Musgrave lab. The photoinitiator was computed using wB97xd/Lanl2dz/CPCM-acetonitrile theory. The f is the oscillator strength and it is proportional to the molar absorptivity. The LANL2DZ is an effective core potential basis set. PCM stands for conductor-like polarizable continuum model which is a commonly used method to model solvation effects, which in this experiment was specifically set to acetonitrile.

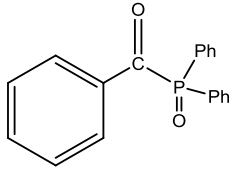
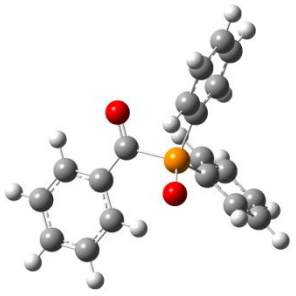
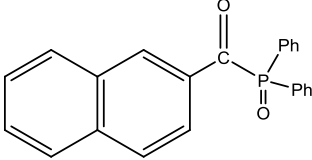
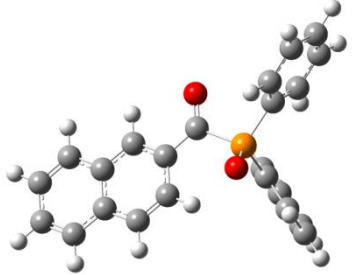
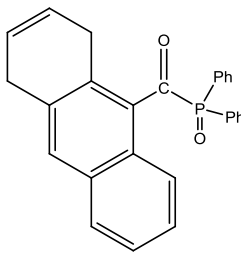
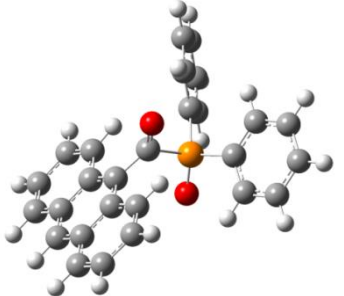
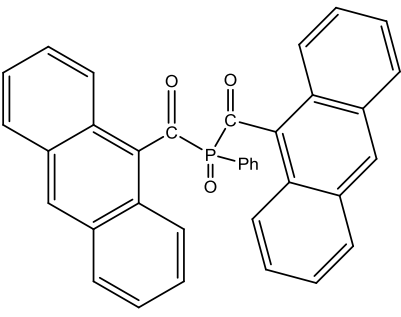
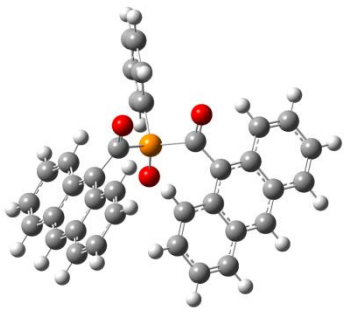
Photoinitiator Structure	Molecular Structure	Computed Lambda Max (λ_{\max})
		$\lambda_{\max, \text{calc}} = 384 \text{ nm}$ $f = 0.0027$
		$\lambda_{\max, \text{calc}} = 386 \text{ nm}$ $f = 0.0031$
		$\lambda_{\max, \text{calc}1} = 390 \text{ nm}$ $f = 0.1622$ $\lambda_{\max, \text{calc}2} = 383 \text{ nm}$ $f = 0.0339$
		$\lambda_{\max, \text{calc}1} = 416 \text{ nm}$ $f = 0.1988$ $\lambda_{\max, \text{calc}2} = 407 \text{ nm}$ $f = 0.0628$ $\lambda_{\max, \text{calc}3} = 392 \text{ nm}$ $f = 0.1563$

Table 1. Quantum chemical, computational prediction of the photoinitiators absorption wavelength using wB97xd/Lan12dz/CPCM-acetonitrile theory.

Results

NMR (^1H , ^{13}C , and ^{31}P)

Nuclear Magnetic Resonance (NMR) spectroscopy was performed on 2-Naphthacene, 9-Anthracene (APO) and 9-Anthracene (BAPO). Integration of the peaks on the ^1H NMR provides a good indication that these photoinitiators were indeed synthesized with minimal impurities still present. With aromatic rings, the aromatic hydrogen normally have chemical shifts in the 7.0-7.4 ppm region and appear as either a broad singlet or complex multiple peaks which occurs for the photoinitiators that were synthesized.

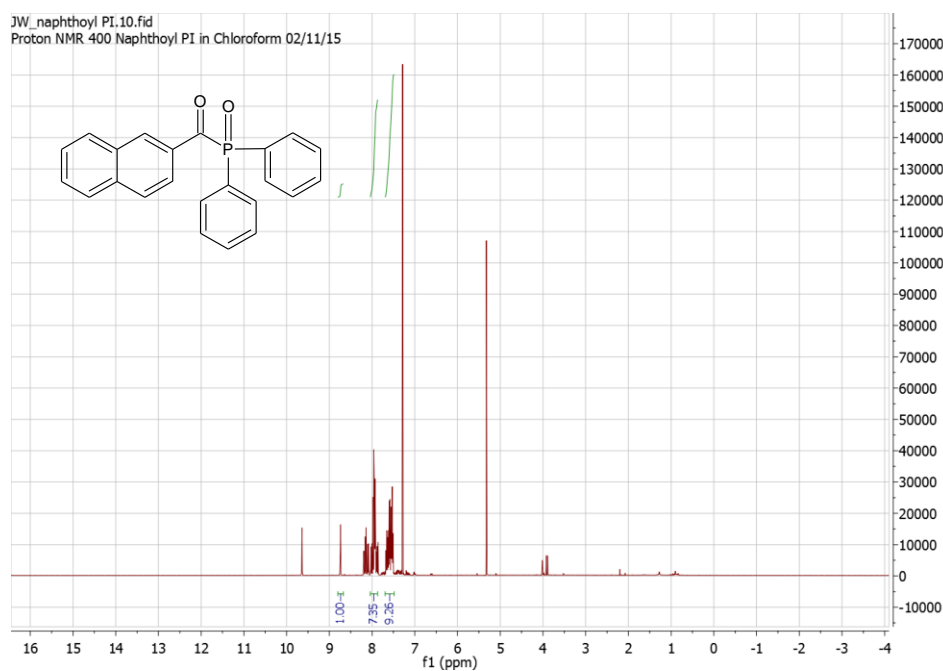


Figure 5. ^1H NMR of 2-Naphthacene (APO) PI in CDCl_3 .

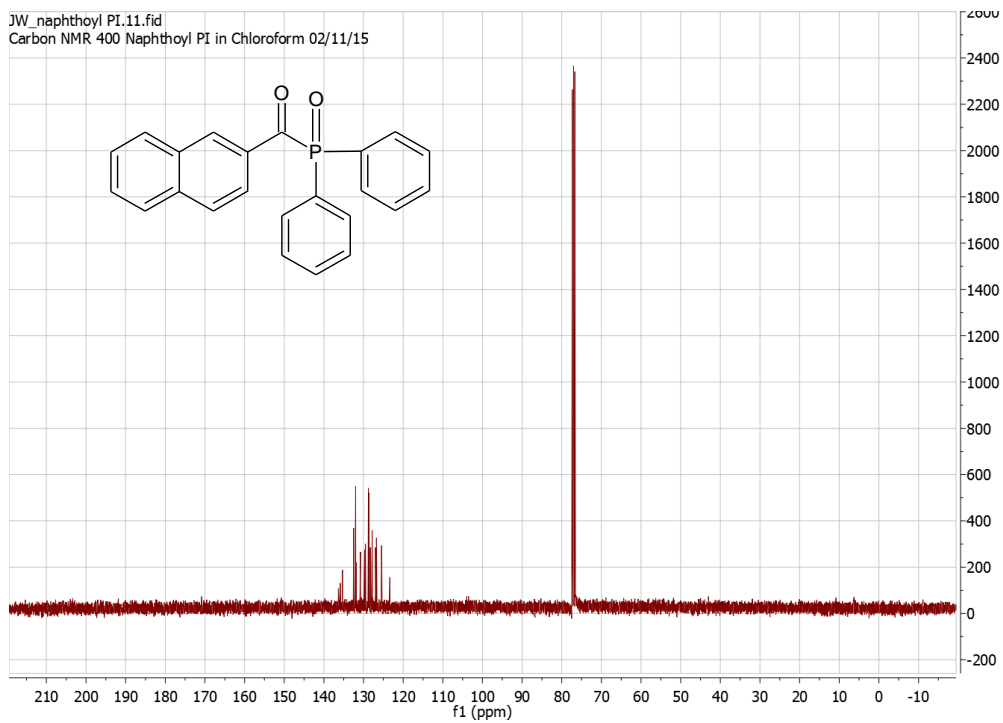
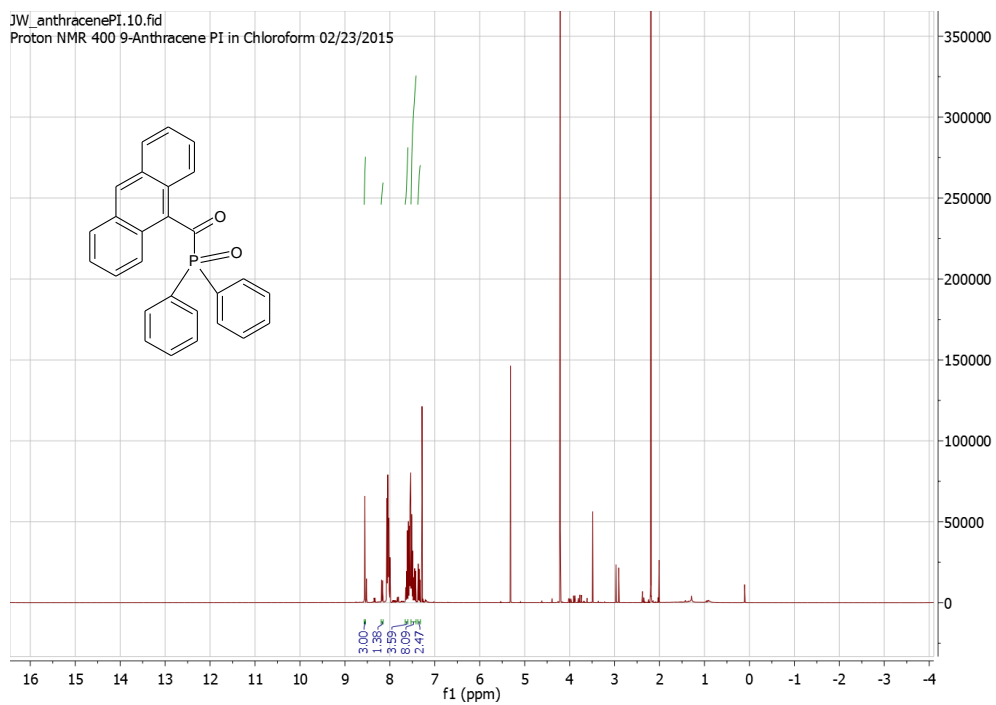
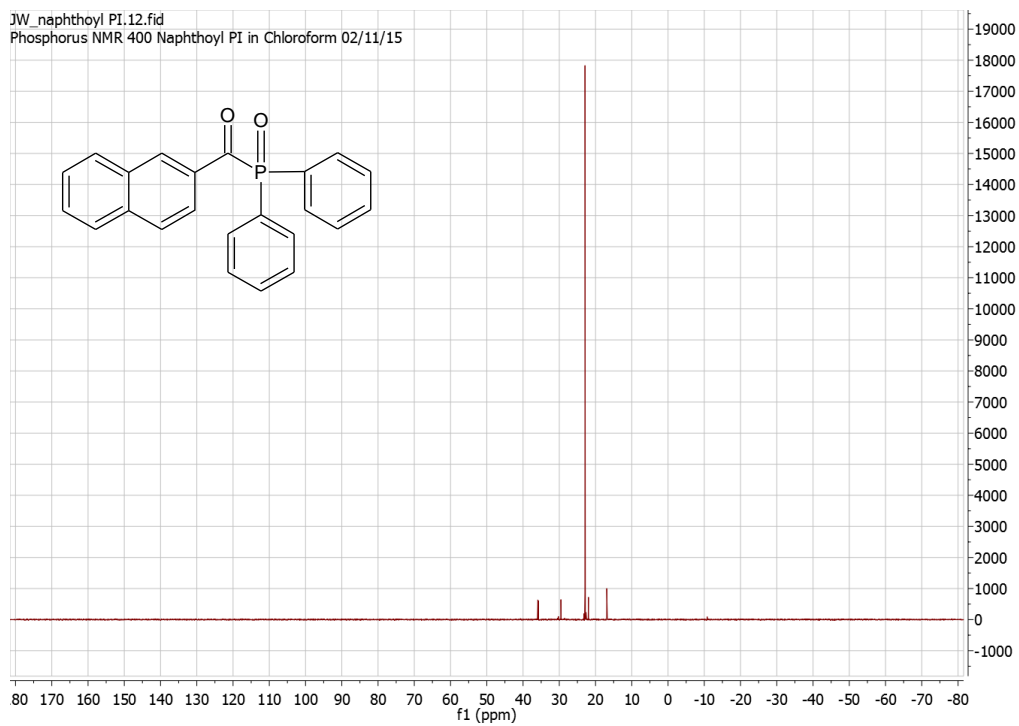


Figure 6. ^{13}C NMR of 2-Naphthacene (APO) PI in CDCl_3 .



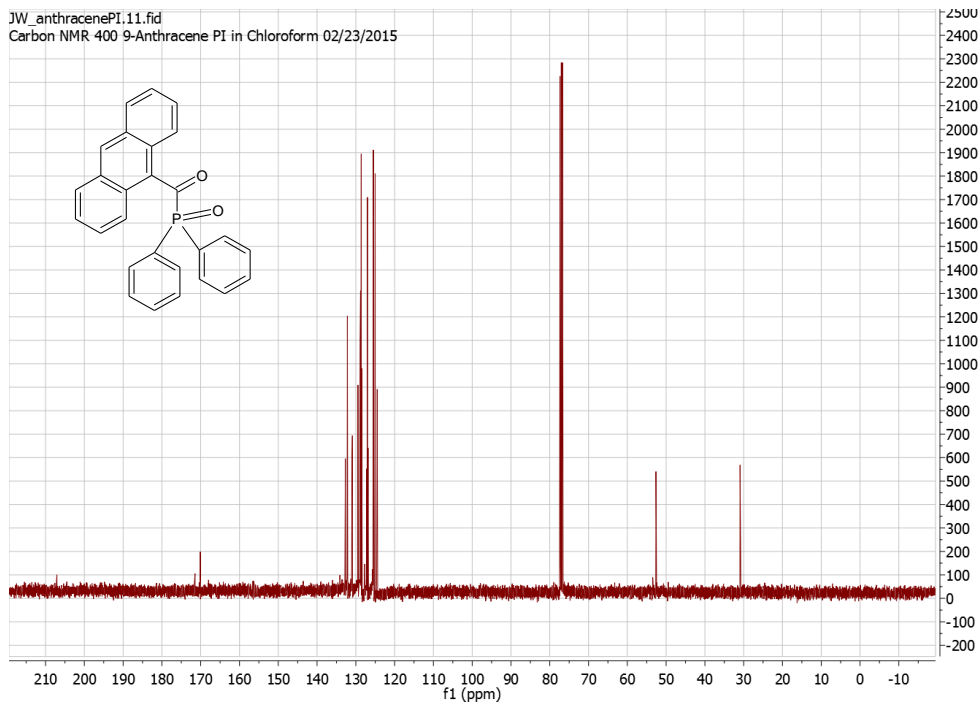


Figure 9. ^{13}C NMR of 9-Anthracene (APO) PI in CDCl_3 .

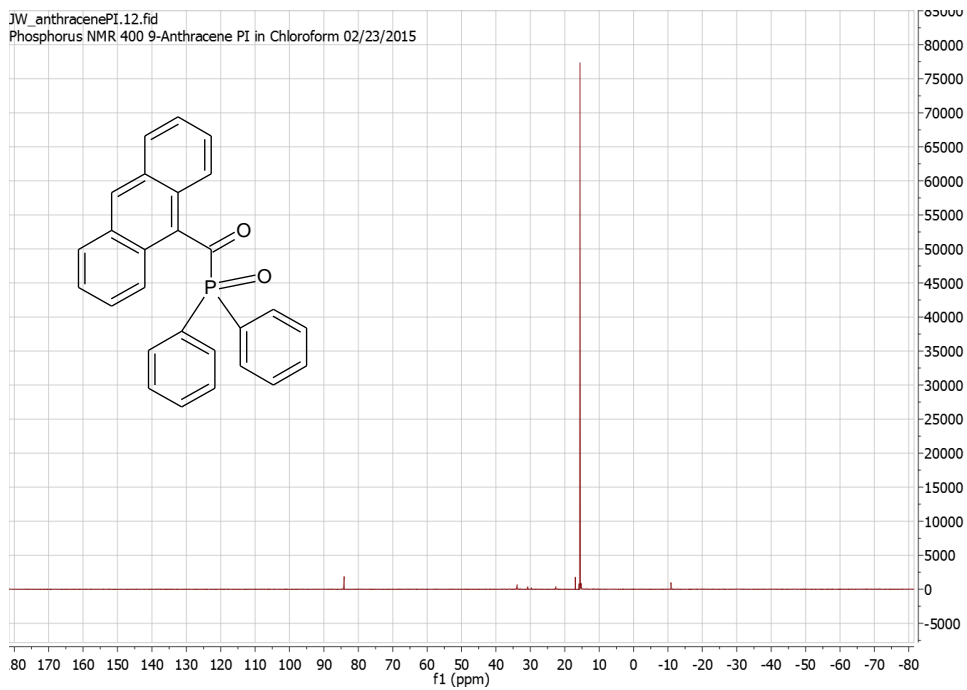


Figure 10. ^{31}P NMR of 9-Anthracene (APO) PI in CDCl_3 .

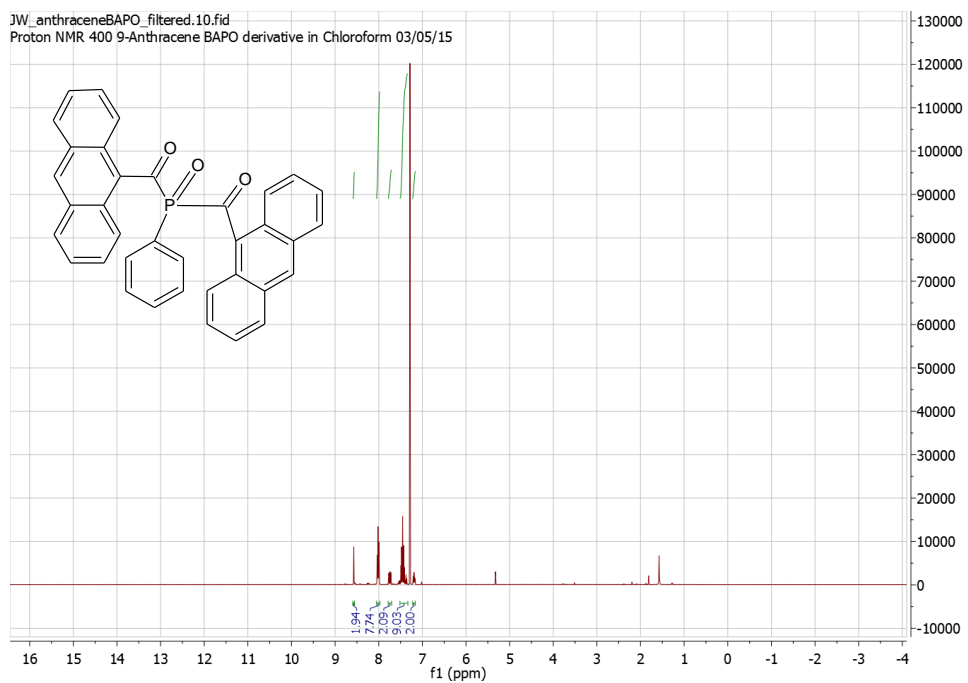


Figure 11. ^1H NMR of 9-Anthracene (BAPO) in CDCl_3 .

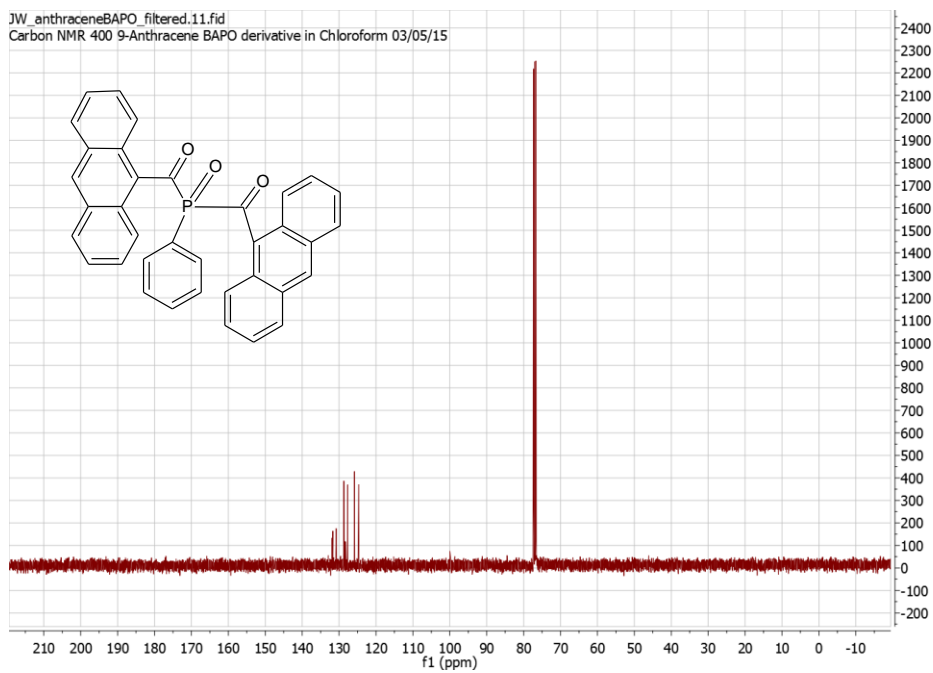


Figure 12. ^{13}C NMR of 9-Anthracene (BAPO) in CDCl_3 .

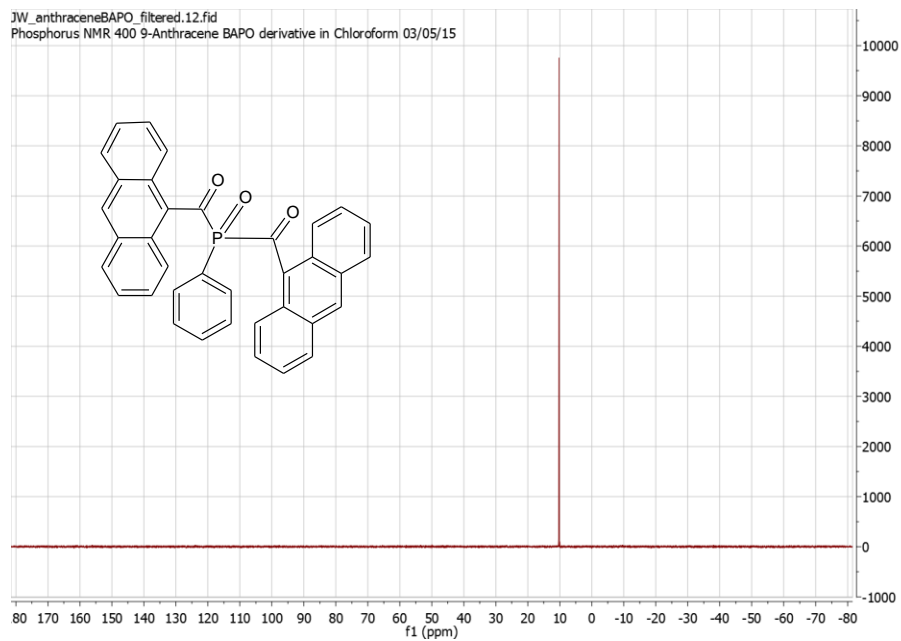


Figure 13. ^{31}P NMR of 9-Anthracene (BAPO) in CDCl_3 .

Mass Spectrometry

Mass Spectrometry is another analytical tool that was used to confirm the synthesis of the designed photoinitiators. Electrospray Ionization was the utilized technique for the analysis of the polar photoinitiators. The advantage of using Electrospray Ionization is that the mass of the sample can be determined with a high accuracy and the instrument is very sensitive to obtain accurate quantitative and/or qualitative result.

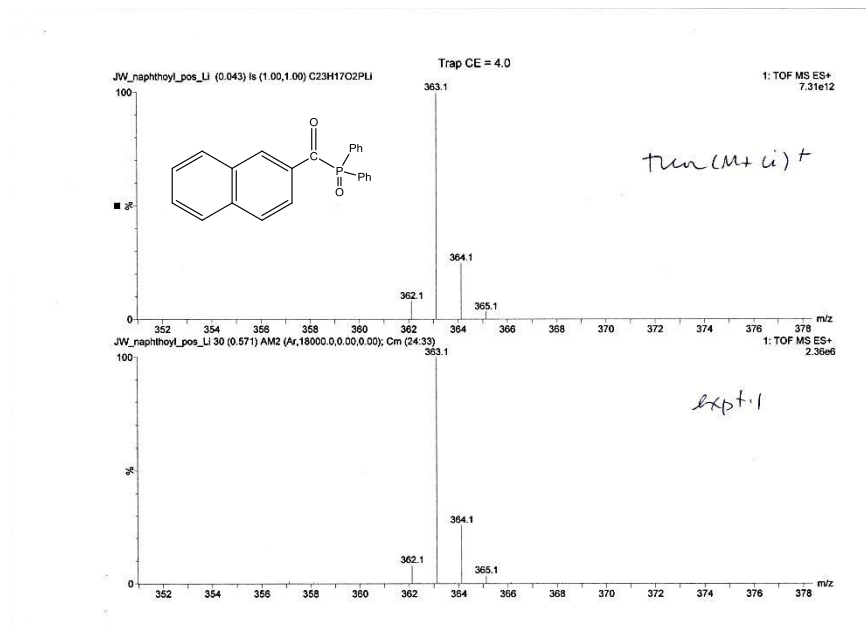


Figure 14. Chemical Ionization Mass Spectrometry with Lithium ion attachment to 2-Naphthacene PI. Theoretical and Experimental Result.

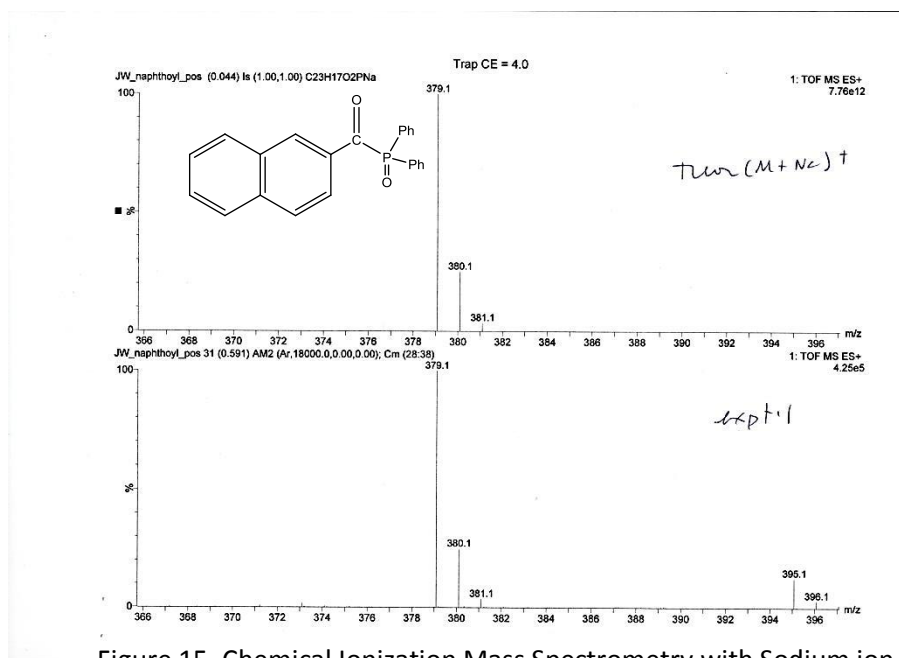


Figure 15. Chemical Ionization Mass Spectrometry with Sodium ion attachment to 2-Naphthacene PI. Theoretical and Experimental Result.

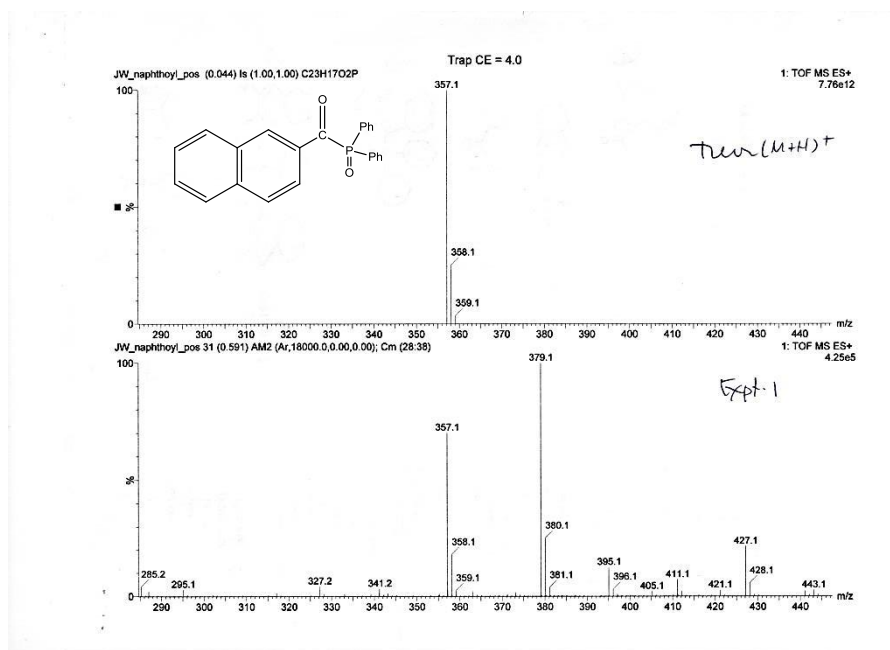


Figure 16. Chemical Ionization Mass Spectrometry with Hydrogen ion attachment to 2-Naphthacene PI. Theoretical and Experimental Result.

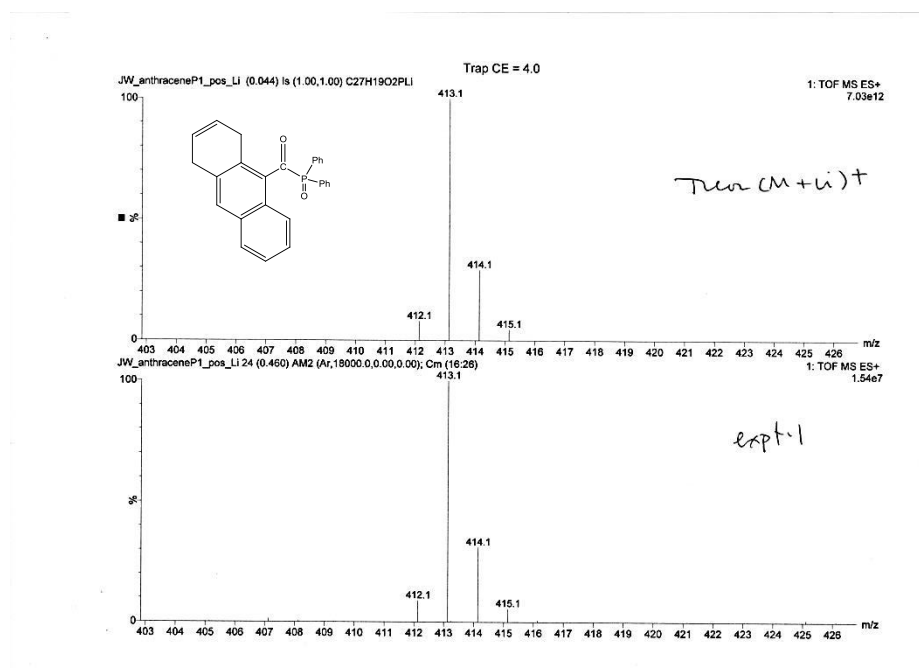


Figure 17. Chemical Ionization Spectrometry with Lithium Ion Attachment to 9-Anthracene (APO). Theoretical and Experimental.

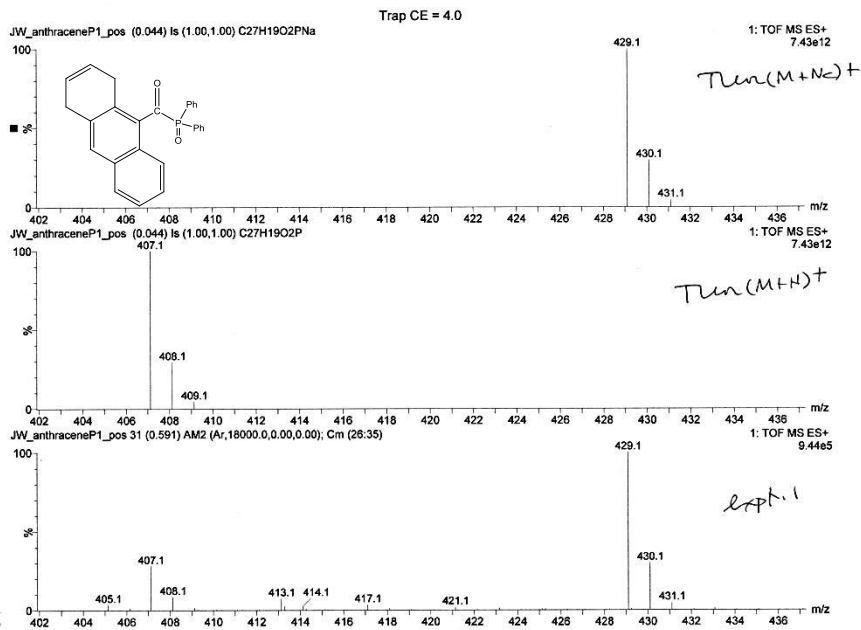


Figure 18. Chemical Ionization Mass Spectrometry with Sodium ion and Hydrogen ion attachment to 9-Anthracene (APO) PI. Theoretical and Experimental Result.

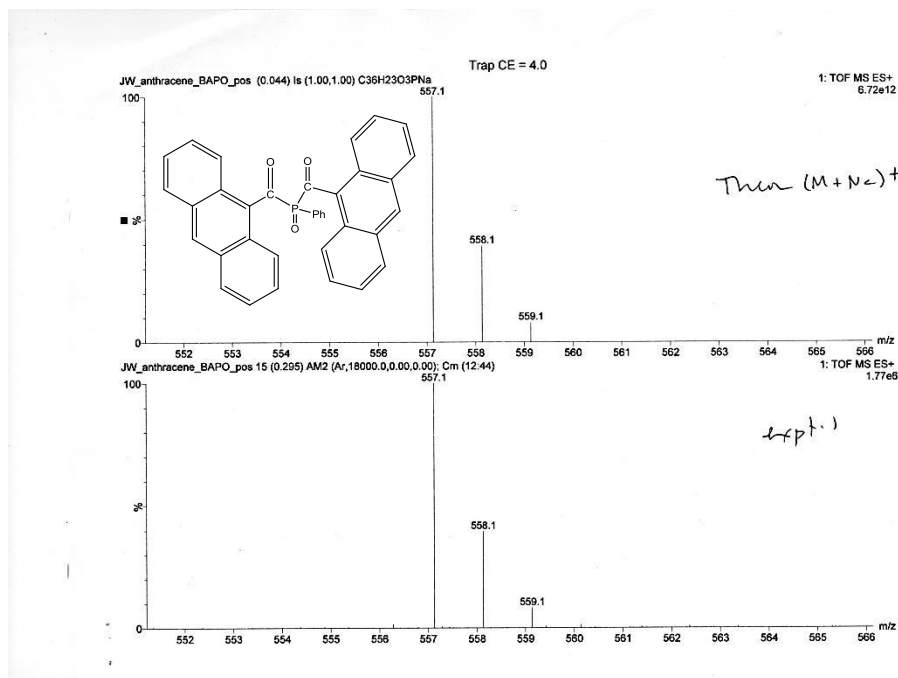


Figure 19. Chemical Ionization Mass Spectrometry with Sodium ion attachment to 9-Anthracene (BAPO) PI. Theoretical and Experimental Result.

UV-Vis Spectroscopy

A UV-visible Absorption Spectrum was measured for each photoinitiator synthesized as well as the control photoinitiators that were commercially bought that serve as the control. Molar Absorptivity or Molar Extinction Coefficient (ϵ) was calculated as:

$$\epsilon = A / cl$$

where A is the absorbance, c is the concentration of the sample in moles/liter, and l is the path length of the cuvette. In this experiment the path length of the cuvette was 0.5 cm. Once the lambda max, λ_{max} , (wavelength of maximum absorbance) of the photoinitiators was read from the spectrum produced, the molar extinction coefficient was calculated by creating a calibration curve of various concentrations of the measured photoinitiator. A best fit line was plotted to which a straight line was produced. The slope of the curve generated is the measured Molar Extinction Coefficient. The Molar Extinction Coefficient of the photoinitiators was calculated in both dichloromethane and acetonitrile.

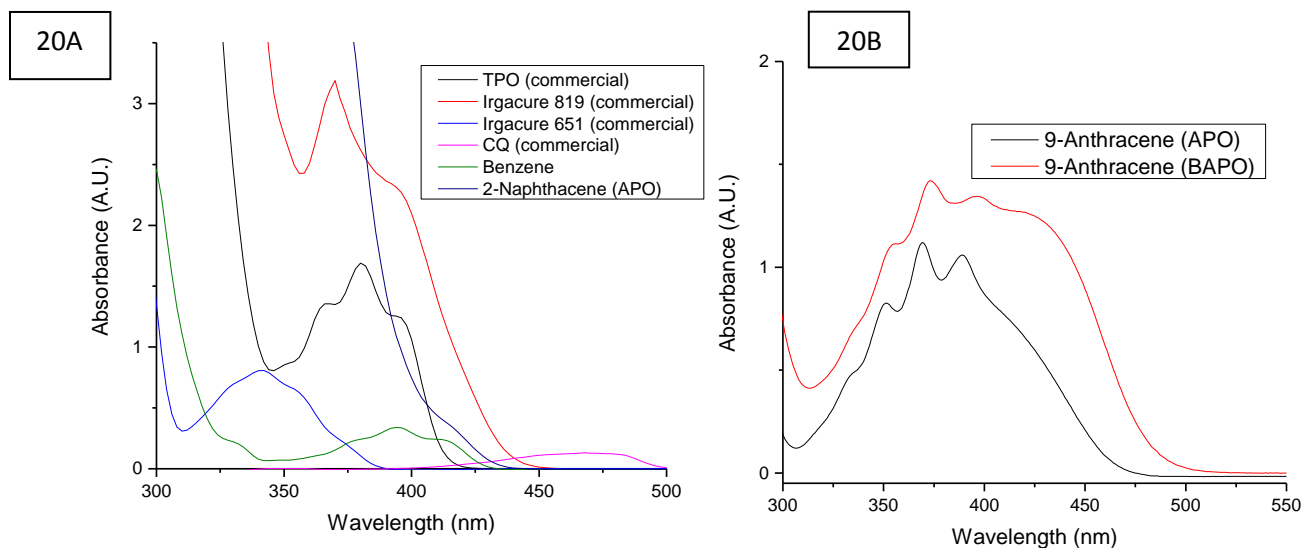


Figure 20. UV-vis spectroscopy of photoinitiators. Figure 20A, the photoinitiators are at 6 mM concentration in DCM using a 0.5 cm path length cuvette. Figure 20B, the photoinitiators are at 4×10^{-1} mM concentration in DCM using a 0.5 cm path length cuvette.

Photoinitiator	Short Name	Classified As	Appearance	UV-vis Spectra (λ_{max} , nm)	Molar Extinction Coefficient in Acetonitrile ($M^{-1} \cdot cm^{-1}$)	Molar Extinction Coefficient in DCM ($M^{-1} \cdot cm^{-1}$)
2,4,6-Trimethyl	TMDPO	APO	White Powder	367, 380, 393	382, 476, 352	426, 528, 392
Benzene	BDPO	APO	Light Yellow Wax	394	311	109.8
2-Naphthacene	NDPO	APO	Light Yellow Powder	420	77.2	90.4
9-Anthracene	ADPO	APO	Bright Yellow Powder	350, 368, 390	3474, 4683, 4398	4225, 5757, 5436
BAPO	IC 819	BAPO	Light Yellow Powder	371,400	1200, 890	1070,704
9-Anthracene	N/A	BAPO	Bright Yellow Powder	373, 400	N/A	7676, 7206
CQ	CQ	Tertiary Amine	Bright Yellow Powder	469	73	42
DMPA	IC 651		White Powder	341	279	258

Table 2. Displays the photoinitiators used and its general appearance as well as the lambda max and molar extinction coefficient associated using two different solvents.

Infrared IR Spectroscopy

A study was carried out in which the homo-photopolymerization of Triethylene glycol diacrylate (TEGDA) was observed and the degree of conversion in the disappearance of the double bond in TEGDA to single bonds was measured. A solution was prepared by dissolving the same mole percent of photoinitiators (0.024 mmoles) in 2.40 mL of TEGDA resulting in a 10 mM solution of each independent photoinitiator. Each photoinitiators kinetics where studied by adding a drop of the solution to a NaCl salt plate and running a series collection and exposing the salt plate to 365 nm filter light. The

lamp was turned on at exactly 1 minute after the beginning of data collection and left on for 30-60 minutes. The experiment was repeated twice at varying light intensity (5 mW/cm^2 and 50 mW/cm^2) and with 400-500 nm filter in the lamp, while all other conditions remained the same.

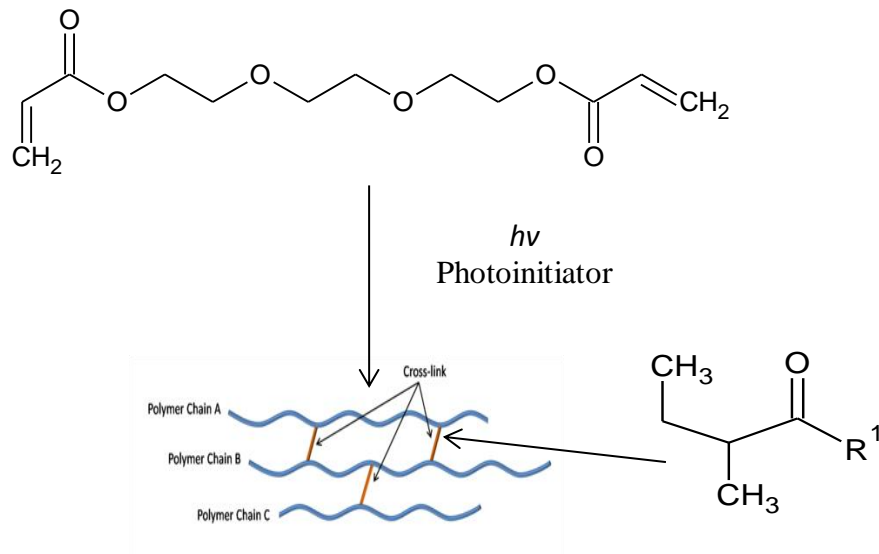


Figure 21 displays a schematic of Triethylene glycol diacrylate (TEGDA) self-polymerizing with the usage of photoinitiators. Once exposed to light, photo-cleavage of the PI will generate free radicals that will promote homo-polymerization of TEGDA to form a highly cross-linked polymer.

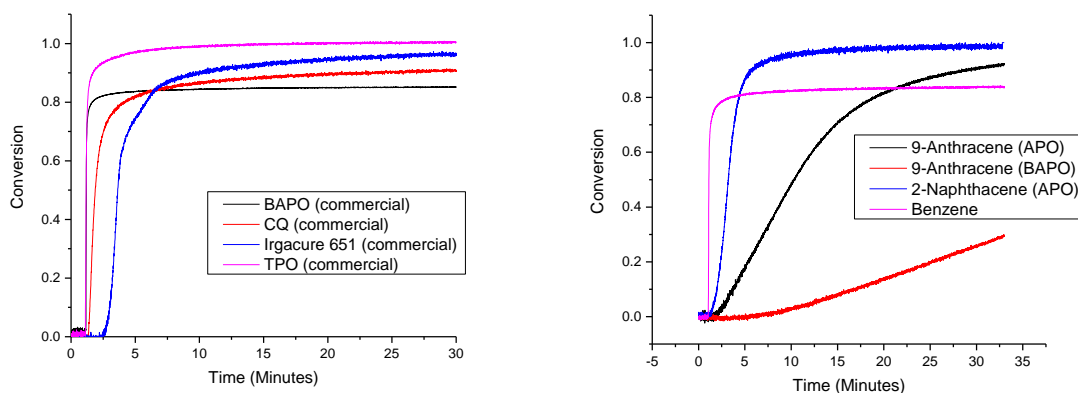


Figure 22. Displays the kinetics of the photoinitiators exposed to 400-500 nm filter light at an intensity of 5 mW . All photoinitiators are dissolved in TEGDA at the same mole percent, 0.024 mmoles in 2.24 mL of TEGDA which equates to 10 mM. Lamp was turned on at exactly 1 minute.

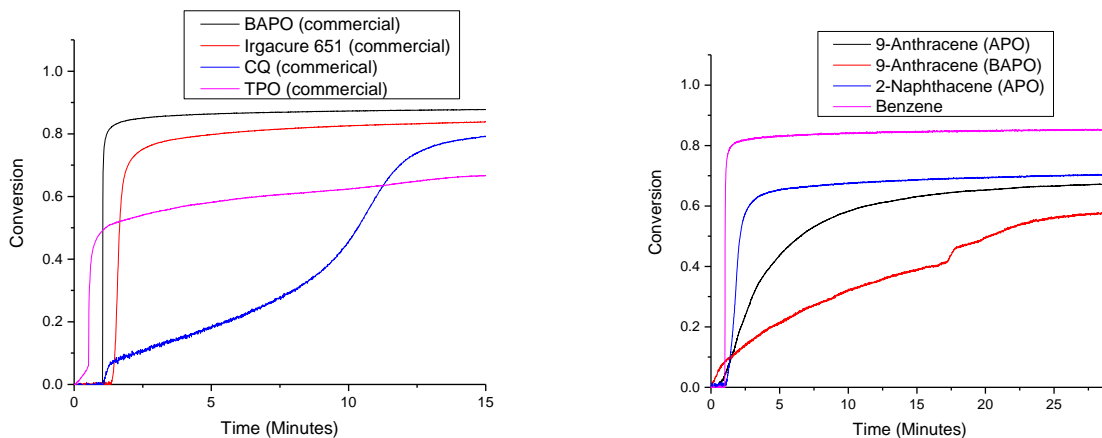


Figure 23. Displays the kinetics of the photoinitiators exposed to 400-500 nm filter light at an intensity of 50 mW. All photoinitiators are dissolved in TEGDA at the same mole percent, 0.024 mmoles in 2.24 mL of TEGDA which equates to 10 mM. Lamp was turned on at exactly 1 minute.

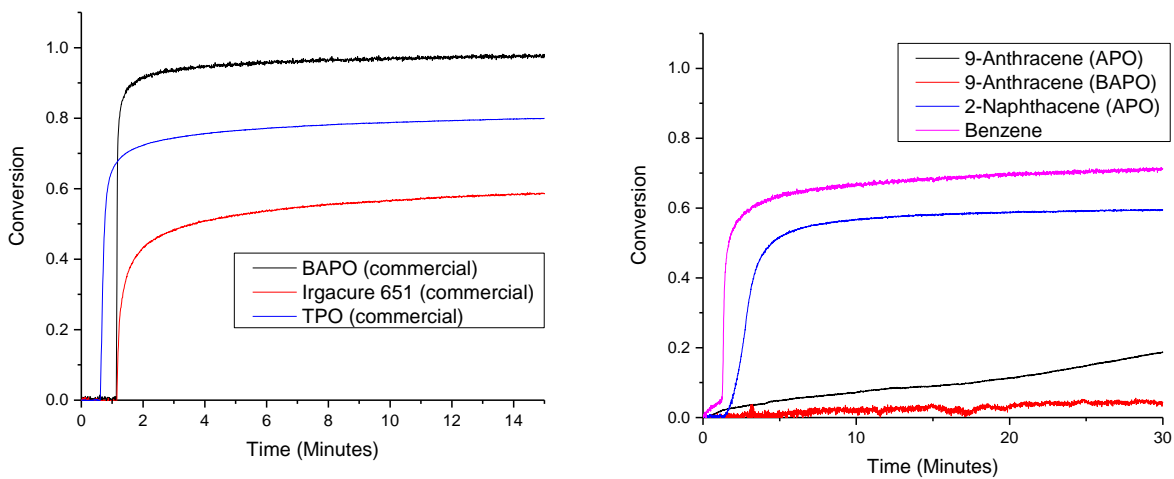


Figure 24. Displays the kinetics of the photoinitiators exposed to 365 nm filter light at an intensity of 5 mW. All photoinitiators are dissolved in TEGDA at the same mole percent, 0.024 mmoles in 2.24 mL of TEGDA which equates to 10 mM. Lamp was turned on at exactly 1 minute.

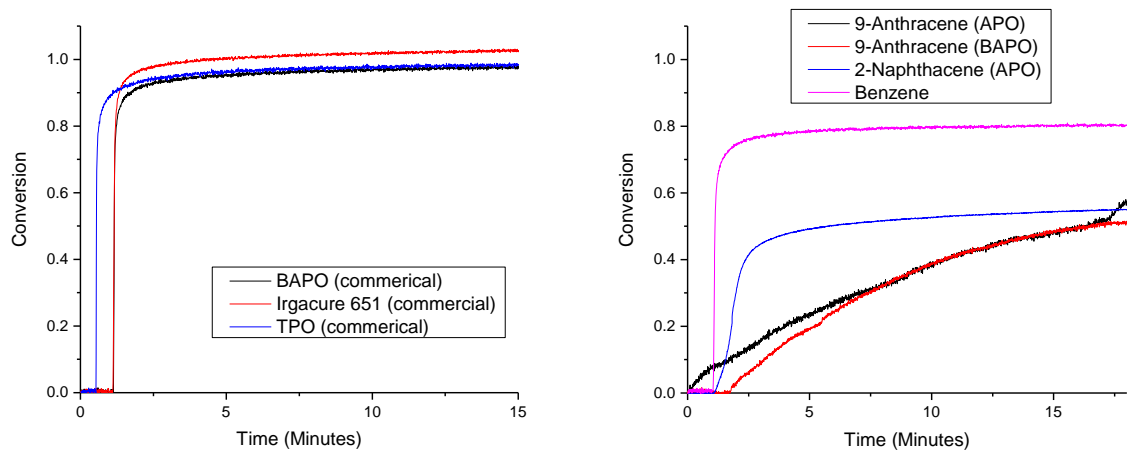


Figure 25. Displays the kinetics off the photoinitiators exposed to 365 nm filter light at an intensity of 50 mW. All photoinitiators are dissolved in TEGDA at the same mole percent, 0.024 mmoles in 2.24 mL of TEGDA which equates to 10 mM. Lamp was turned on at exactly 1 minute.

Real Time UV-vis

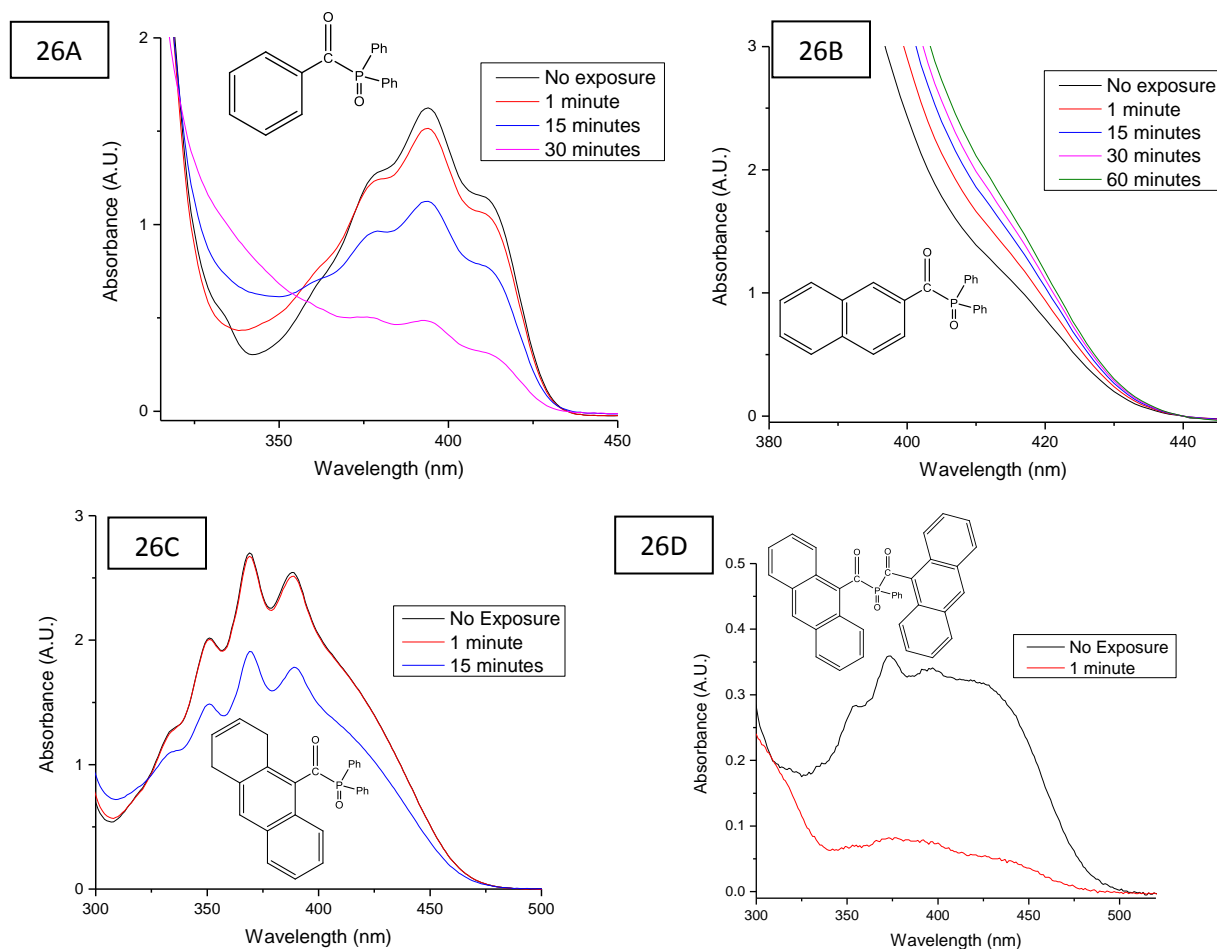


Figure 26. Displays the real time UV-vis results of the photoinitiators exposed to LED Blue Light Lamp (~ 450 nm) at 80 mW/cm^2 . All UV-vis measurements were performed in a 0.5 cm path length cuvette and samples dissolved in DCM at concentrations A) 33 mM, B) 28 mM, C) 1×10^{-1} mM, and D) 1×10^{-5} mM.

Photo-bleaching

Photo-bleaching is the measurement of the absorbance of the photoinitiator decreasing by being exposed to illumination over time. The experiment conducted involves exposing a certain measured concentration of photoinitiators dissolved in a solvent to LED Dental Curing Light that has a selected emission wavelength of 450 nm that tails to 420 nm and 480 nm.

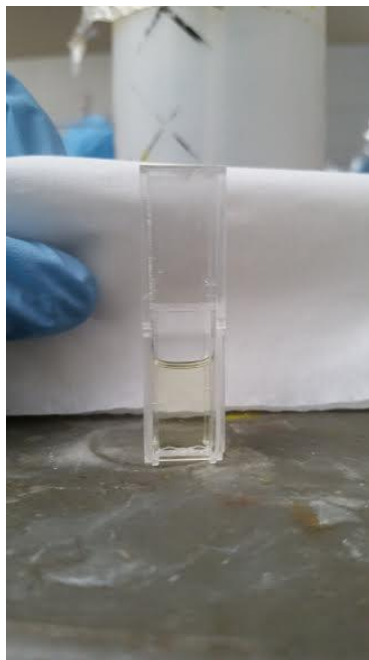
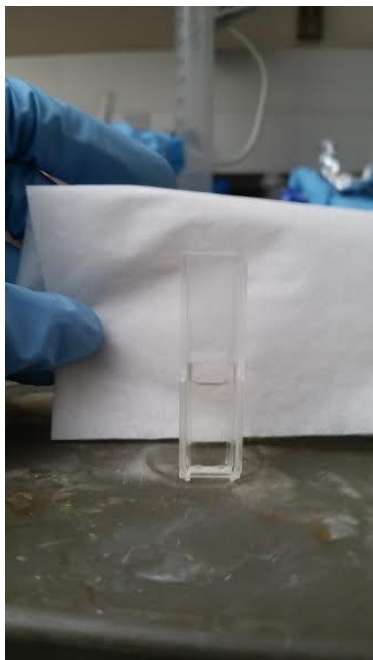


Image 1. Displays 2-Naphthacene PI. A) before exposure, B) after exposure to 80 mW/cm^2 light intensity of LED blue Lamp.



Image 2. Displays 9-Anthracene (APO) PI. A) before exposure, B) after exposure to 80 mW/cm^2 light intensity of LED blue Lamp.

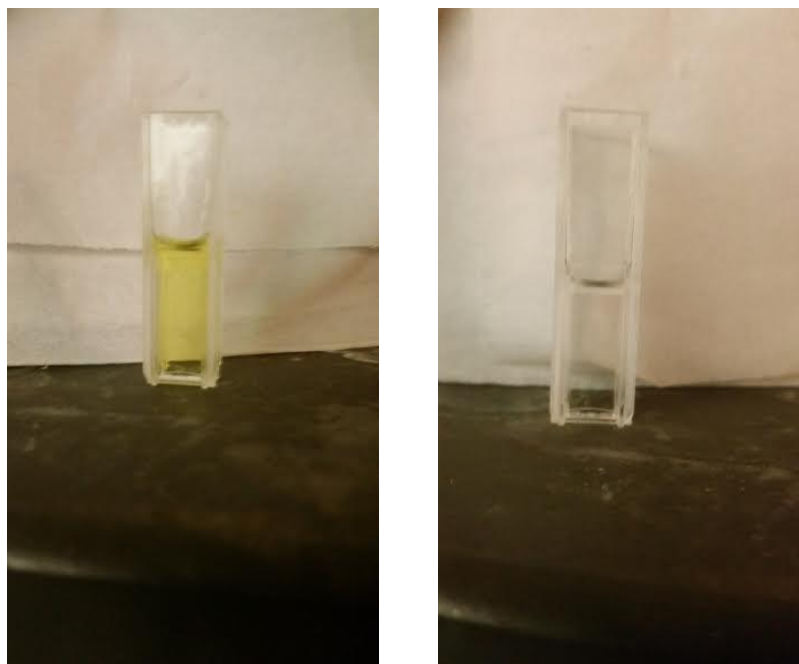


Image 3. Displays 9-Anthracene (BAPO) PI. A) before exposure, B) after exposure to 80 mW/cm² light intensity of LED blue Lamp.

Discussion

The goal of this research is to design and synthesize new photoinitiators that are red-shifted from conventional UV absorption to Visible light absorption. The computationally designed 2-naphthacene (APO), 9-Anthracene (APO), and 9-Anthracene (BAPO) were computed to have a λ_{max} of 386, 390 and 383, and 416, 407, and 392 nm, respectively. In addition, a general proof of concept was expected to be demonstrated when the overall aromaticity of the molecule is increased because of the importance of conjugation. Increasing conjugation leads to the HOMO and LUMO orbitals approaching closer which would increase the wavelength as well as the molar extinction coefficient.

In order to validate that 2-naphthacene (APO), 9-Anthracene (APO), and 9-Anthracene (BAPO) were indeed synthesized, two analytical techniques were conducted, Nuclear Magnetic Resonance (NMR) imaging and Mass Spectrometry. The results indicate that there is a high reasonable possibility that these

photoinitiators were synthesized. The integration of the peaks around 7.0-9.0 ppm on the ^1H NMR roughly corresponds to the total protons on the desired photoinitiator. In addition, the ^{31}P NMR shows a single phosphorus peak indicating that the starting material, Methyl diphenylphosphinite, is no longer present which would have a peak at 120 ppm. In order to further promote possibility, the samples were submitted to a mass spectrometry facility. The facility used the technique of Electrospray Ionization where it was theoretically predicated that 2-Naphthacene $[\text{M}+\text{Li}]^+$, $[\text{M}+\text{H}]^+$, and $[\text{M}+\text{Na}]^+$ would be 363.1 m/z, 357.1 m/z, and 379.1 m/z, respectively. It was theoretically predicated that 9-Anthracene (APO) $[\text{M}+\text{H}]^+$, $[\text{M}+\text{Li}]^+$, and $[\text{M}+\text{Na}]^+$ would be 407 m/z, 413 m/z, and 429 m/z, respectively. It was lastly predicated that 9-Anthracene (BAPO) $[\text{M}+\text{Na}]^+$ would be 557.1 m/z. All of experimental results match to the theoretical predictions. 9-Anthracene (BAPO) polarity greatly reduced due to the twisting of the aromatic 3-ring creating a barrier on the polar carbonyl and phosphorus atom which explains why $[\text{M}+\text{Li}]^+$ and $[\text{M}+\text{H}]^+$ could not be adducted properly to the molecule.

Once the photoinitiators were synthesized and relatively pure, a UV-vis spectroscopy measurement was conducted. Table 2 provides the measured molar extinction coefficient (ϵ) of the observed λ_{max} of the PIs. 9-Anthracene (BAPO) was not soluble in acetonitrile so (ϵ) was conducted using dichloromethane. Granted dichloromethane is a non-polar solvent while acetonitrile is a polar aprotic solvent, the polarity index of dichloromethane was 3.1 and acetonitrile 5.8. Therefore, the polarity was slightly reduced with the exchange of solvent allowing 9-Anthracene (BAPO) to dissolve and measure (ϵ). As expected, a general proof of concept was demonstrated by (ϵ) greatly increasing almost 60x from 2-Naphthacene (APO) to 9-Anthracene (APO). Figure 20A demonstrates that increasing the conjugation of the aromatic ring from Benzene PI to 2-Naphthacene shows a small red shift occurring. Figure 20B demonstrates that the creation of 9-Anthracene (BAPO) lead to an increase in (ϵ) compared to 9-Anthracene (APO). The experimental λ_{max} of 2-Naphthacene (APO), 9-Anthracene (APO), and 9-Anthracene (BAPO) were shown as 420 nm, (350, 368, and 390) nm, and (373 and 400) nm, respectively. This slightly deviates from the computational studies described previously where it was predicated that 2-Naphthacene (APO), 9-Anthracene (APO), and 9-Anthracene (BAPO) would have a λ_{max} at 386 nm, (390

and 383) nm, and (392, 407, and 416) nm, respectively. The experimental values are within a reasonable range from the computational method.

The next experimental investigation conducted was to see if increasing the size of the aromatic ring stabilized the overall molecule to the point where α -cleavage would be infringed resulting in no radical production. In order to demonstrate this all control photoinitiators and newly designed photoinitiators were dissolved at the same mole percent in Triethylene Glycol Diacrylate (TEGDA), roughly equating to 10 mM. It is essential to keep the mole percent equivalent so that the same number of molecules of each photoinitiator is present so the efficiency of the photoinitiators can be compared. A set of experiments were conducted so that a sample of each 10 mM sample of photoinitiator were tested using 365 nm filter light and changing the parameter of light intensity from 5 mW/cm² to 50 mW/cm². The experiment was conducted a second time where the filter lamp was replaced using a 400-500 nm filter light to test the photoinitiator activity exposed to visible light. As Figures 22-25 demonstrates, all newly synthesized photoinitiators did indeed undergo cleavage to create radicals that helped with the homo-polymerization of TEGDA to form a high cross-linked polymer. Unfortunately, increasing the aromatic ring size did lead to a decrease in the conversion and efficiency of the photoinitiator. Figure 23 shows the control photoinitiators and the newly synthesized photoinitiators exposed to 400-500 nm filter light at 50 mW/cm² intensity. In comparison to the control, the new photoinitiators took roughly 30 minutes before conversion began to plateau while the commercial brand photoinitiators took roughly 2-15 minutes. It is apparent that as the ring size increases from benzene, 2-Naphthacene (APO), to 9-Anthracene (APO) the conversion drops from 80%, 63%, 60%, and 50%, respectively. This suggests that increasing the size of the ring stabilized the radicals which prevented the photoinitiators from being fast and efficient in homo-polymerization of TEGDA. The same result can be shown with the exposure of 365 nm filter light at 50 mW/cm², Figure 25. The increase in the size of the aromatic ring leads to a conversion drop from 80%, 42%, and 40% within 15 minutes. This indicates that the new photoinitiators (2-Naphthacene (APO), 9-Anthracene (APO), and 9-Anthracene (BAPO)) are better photoinitiators in the visible light region where polymerization occurs faster. In addition, a greater conversion and efficiency

was demonstrated of the new photoinitiators in the visible light region in comparison to UV light exposure.

The last set of experimental investigation performed was to demonstrate that the exposure of LED Dental Curing Lamp at 80 mW/cm^2 would initiate the formation of radicals by observing the absorbance in the visible light region decreasing. In addition, the images that follow display the photo-bleaching effects that result. As Figure 26 demonstrates, radicals do indeed generate with the exposure of 80 mW/cm^2 LED lamp at least for Benzene, 9-Anthracene (APO), and 9-Anthracene (BAPO). Interestingly 2-Naphthacene (APO) absorbance increases in the visible light region. Why this occurs is a mystery and through discussion with graduate Chern-Hooi Lim and Dr. Alan Aguirre, it is speculated that the radicals are possibly recombining to form another molecule that has a greater absorbance in the visible light region. This is demonstrated in photo-bleaching image 1. At first dissolving roughly 30 mM of 2-Naphthacene in DCM lead to transparent, water-like appearance. However, after exposure to the LED lamp an apparent yellow tint began to form. This supports why the absorbance is increasing due to the color change of the solution. What is interesting enough is that 9-Anthracene (BAPO) appears to generates more radicals with the exposure to the LED lamp compared to 9-Anthracene (APO) even though through the kinetics experiment 9-Anthracene (APO) was faster in homo-polymerization TEGDA. It is not validated whether or not more radicals are indeed generated but it is speculated. This result may possibly demonstrates that 9-Anthracene (APO) generates less stable radicals while 9-Anthracene (BAPO) the radicals are more stable and therefore less reactive. The photo-bleaching image 3 of 9-Anthracene (BAPO) shows the complete conversion from a yellow solution to completely transparent.

Conclusion

To summarize, the synthesis of the new photoinitiators (2-Naphthacene (APO), 9-Anthracene (APO), and 9-Anthracene (BAPO)) demonstrate a proof of concept that increasing the conjugation of the ring lead to a red-shift of the wavelength into the visible light region as well as increasing the molar

extinction coefficient (ϵ) based on UV-vis spectroscopy. However, the π - π^* may have been red-shifted leading to high absorptivity but how much of the red-shift is due to the n - π^* needs to be considered and further investigated. Both analytical tools that comprised of NMR spectroscopy and mass spectroscopy give a good indication that these new photoinitiators were synthesized with possible minimum impurity. However, the IR spectroscopy results demonstrate that increasing the size of the aromaticity of the ring leads to a decrease in the efficiency of the photoinitiators radical activity due to the stabilization of the radical. This result is further confirmed in the real time UV-vis which shows 9-Anthracene (BAPO) generating what appears to be more radicals in a faster amount of time. Within a minute the λ_{\max} decreased by about 80% with exposure to 80 mW/ cm² of dental curing light. However, IR kinetic study displays slow rate of homo-polymerization of TEGDA. In comparison, 9-Anthracene (APO) the λ_{\max} decreased to 30% within 15 minutes. The real time UV-vis study of 9-Anthracene (APO) appears to show less radicals being produced but the IR kinetic study demonstrates that the radicals are less stable and result in a faster homo-polymerization of TEGDA. Most of the novel photoinitiators display photo-bleaching capability except for 2-Naphthacene (APO) which would be less ideal in the usage of dental composites due to poor cosmetic appearance. Therefore, the search for a highly efficient long-wavelength photoinitiator is still being investigated, however; based on the knowledge extracted, increasing aromaticity narrows the π - π^* transition which leads to an increase in long-wavelength absorption. In order to create an efficient long-wavelength photoinitiator, the π - π^* transition needs to decrease but the radicals have to be less stabilized.

Future Scope

It has been demonstrated that free radicals are stabilized by increased aryl conjugation due to increase in resonance. A possible new direction in this research which would maintain long-wavelength absorption and molar extinction coefficient but destabilize the free radicals is to include electron withdrawing groups on the aromatic ring. The electron withdrawing groups could remove the electron

density making the free radical less stable. However, there may be a slight cost when adding electron withdrawing groups such as a decrease in the molar extinction coefficient. Another possibility is to change the aromatic structure itself by focusing less on the benzene construct but rather such as a heterocyclic structure such as Pyridine, Pyran, or Thiopyran. In addition, there is the possibility of incorporating multiple heteroatoms. These heteroatoms can possibly display the same effects as including electron withdrawing groups which is to withdraw electron density to form less stable radicals.

References

- 1) de Dios, Angel C. (n.d.) Particle in a Box. Retrieved March 26, 2015, from <http://bouman.chem.georgetwon.edu/S02/lect13/lect13.htm>.
- 2) Fouassier, Jean Pierre and Lalevee, Jacques. (2012). Photoinitiators for Polymer Synthesis: Scope, Reactivity, and Efficiency. Wiley-VCH, Weinheim, Germany. Print.
- 3) Gorsche, Christian, Griesser, Markus, Hametner, Christian, Ganster, Beate, Moszner, Norbert, Neschadin, Dmytro, Rosspeinter, Arnulf, Gescheidt, Georg, Saf, Robert, and Liska, Robert. (2014) New Generation of Highly Efficient Long-Wavelength Photoinitiators for Dental Restorative: From Research to Application. *Radtech UV & EB*, Vienna, Austria
- 4) Hristova, Daniela. (2005). Kinetic Studies of Radical Reactions using Time-Resolved EPR. (Electronic Thesis or Dissertation). Retrieved from https://doc.unibas.ch/225/1/DissB_7165.pdf
- 5) Kilian, Robert J. (1981). The Application of Photochemistry to Dental Materials. Biomedical and Dental Applications of Polymers, *Polymer Science and Technology*, 14, 411-417.
- 6) Linden, Lars-Ake. (1993). Applied Photochemistry in Dental Science. *Journal of Chemical Sciences*, 105(6): 405-419.
- 7) Musanje L, Ferracane, JL, Sakaguichi, RL. (2009). Determination of the Optimal Photoinitiator Concentration in Dental Composites Based on Essential Material Properties. *Dental Materials*, 25(8); 994-1000.
- 8) Neumann, Miguel G. (2005). Molar Extinction Coefficients and the Photon Absorption Efficiency of Dental Photoinitiators and Light Curing Units. *Journal of Dentistry*, 33; 525-532.
- 9) Schafer, Katherine J., Hales, Joel M., Balu, Mihaela, Belfield, Kevin D., Van Stryland, Eric W., and Hagan, David J.(2004). Two-Photon Absorption Cross-Sections of Common Photoinitiators. *Journal of Photochemistry and Photobiology A: Chemistry*, 162; 497-502.

- 10) Schuster, M., Chen, S.X., Liska, R., Rumpler, M. (2005). Development of Biodegradable Photopolymers for Bone Tissue Engineering. *RadTech Europe Conference & Exhibition*, Vienna, Austria.
- 11) Shinamura, Shoji, Osaka, Itaru, Miyazaki, Eigo, and Takimiya, Kazuo. (2011). Air Stable and High-Mobility Organic Semiconductors Based on Heteroarenes for Field-Effect Transistors. *The Japan Institute of Heterocyclic Chemistry*, 83(6); 1187-1204.
- 12) Sobhi, H. (2008). Synthesis and Characterization of Acylphosphine Oxide Photoinitiators. (Electronic Thesis or Dissertation). Retrieved from <https://etd.ohiolink.edu>.
- 13) Soderberg, Tim. (n.d.). Section 4.3: Ultraviolet and Visible Spectroscopy. Retrieved March 27, 2015, from http://chemwiki.ucdavis.edu/Organic_Chemistry/Organic_Chemistry_With_a_Biological_Emphasis/Chapter_04%3A_Structure_Determination_I/Section_4.3%3A_Ultraviolet_and_visible_spectroscopy.
- 14) Sommerlade, Reinhard H, et al. (2004). Process for Preparing Acylphosphine and Derivatives There of No. 7439401. Ciba Specialty Chemicals Corporation. Patent.
- 15) Spichty, Martin, Turro, Nicholas J., Rist, Gunther, Birbaum, Jean-Luc, Dietliker, Kurt, Wolf, Jean-Pierre, Gescheidt, Georg. (2001). Bond Cleavage in the Excited State of Acyl Phosphine Oxides Insight on the Role of Conformation by Model Calculations: A Concept. *Journal of Photochemistry and Photobiology A: Chemistry*, 142; 209-213.
- 16) 3M ESPE. (2002). Retrieved March 27, 2015, from <http://multimedia.3m.com/mws/media/1680930/led-technology.pdf>